Journal of Materials Chemistry C

Accepted Manuscript

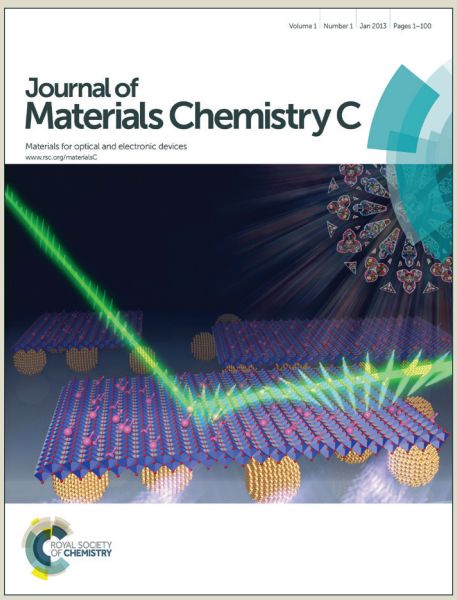

ROYAL SOCIETY OF CHEMISTRY

www.rsc.org/materialsC

Cite this: DOI: 10.1039/c0xx00000x

www.rsc.org/xxxxxx

ARTICLE TYPE

Enhanced nonlinear optical properties of nonzero-bandgap graphene materials in glass matrices

Xiaoqing Zheng,[a] Miao Feng,[a] Zhongguo Li,[b] Yinglin Song[b] and Hongbing Zhan,*[a]

Received (in XXX, XXX) Xth XXXXXXXXX 20XX, Accepted Xth XXXXXXXXX 20XX

DOI: 10.1039/b000000x

The third-order nonlinear optical (NLO) properties of the nonzero-bandgap graphene materials, including graphene oxide nanosheets, graphene oxide nanoribbons, graphene quantum dots, and corresponding hybrid glasses, were investigated using ns and ps Z-scan at 532 nm. The observed nonlinear absorption effects were affected by the laser duration. Reverse saturable absorption was observed in the ns regime, while saturable absorption dominated in the ps regime. The NLO performance was enhanced in the hybrid glasses. These findings open up new possibilities for the practical application of graphene materials in the NLO field.

Graphene is a versatile carbon nanomaterial that has attracted the interest of physicists because of its unique electronic band structure. Theoretically, graphene consists of a single layer of hexagonally arranged sp^2-hybridized carbon atoms, and is a zero-bandgap material. To promote the application of graphene in photonics, such as fast optical communications, all-optical switches, optical limiters, and saturable absorbers, much effort has been dedicated to manipulating and controlling the photoelectric performance by increasing the bandgap.[1-4] These efforts can be divided into two approaches: the first approach is to physically or chemically reduce the connectivity in the π-electronic network via sp^3-hybridized separation,[5,6] while the second is to break the large graphene sheets into nanoscale pieces that show edge confinement or quantum confinement effects.[7,8] Investigations of the nonlinear optical (NLO) performance of graphene materials have been successfully carried out using both of these approaches.[9-13] Typical third-order NLO phenomena, including saturable absorption (SA) and reverse saturable absorption (RSA), have been observed in these graphene materials when they are subjected to laser irradiation. For SA, the absorption coefficient decreases with increases in the incident intensity, as a consequence of Pauli blocking. In contrast, the absorption coefficient follows an opposite trend for RSA, such as two-photon absorption (TPA) and free carrier absorption (FCA).

The nonlinearity of composite materials is strongly affected by the matrix, and can be enhanced by choosing a matrix with a low dielectric constant; examples of such matrices are silicate glasses[14] and polymers.[15-19] In that view, the main aim of the present work was to perform a systematic investigation of the nonlinear optical properties of nonzero-bandgap graphene materials, and the correlation between these properties and the matrices. In our previous paper,[14] we have studied the NLO effects of two-dimensional graphene oxide nanosheets (GONSs), one-dimensional graphene oxide nanoribbons (GONRs) and corresponding hybrid glasses in ns regime. The morphology-dependent and matrix enhanced NLO effects were discovered. However, the NLO properties were simply studied under ns laser pulse, and the relationships of bandgap and morphology were not presented. In order to systematically investigate the effect of morphology, matrix and laser duration on the NLO performance of graphene materials, in this communication, we studied the third-order NLO properties of nonzero-bandgap graphene materials with different morphology and their hybrid glasses using the ns and ps Z-scan technique. Zero dimensional graphene quantum dots (GQDs) were prepared. The silicate glass matrix was chosen because of its low dielectric constant, high transparency, and highly effective solidification effect on the homogeneous graphene suspensions; these properties increase the potential for the practical application of graphene materials in the NLO field.

The GONSs and GONRs were prepared by Hummers method from graphite powder and unzipping mutiwalled carbon nanotubes as described in our previous work.[14] The GQDs were prepared from GONSs by hydrothermal route. The raw GONSs (100 mg) were purified by hydrazine hydrate reduction and oxidizing using concentrated H_2SO_4 and HNO_3, followed by ultrasonic treatment for 15-20 h. The mixture was filtered and the filter cake was re-suspended in deionized water (40 mL). The pH was tuned to 8 using NaOH. The suspension was transferred to a autoclave and treated at 200℃ for 10 h. The brown filter solution was further dialyzed in a dialysis bag (retained molecular weight: 3500 Da) overnight, and finally the GQDs were obtained. The GONS, GONR and GQD hybrid glasses were fabricated using sol-gel method. The process was described in detail previously.[14] The doping concentration was 10 mg, 10 mg and 3.6 mg to 1 mol SiO_2, respectively.

The morphology of graphene materials was analyzed by an FEI Tecnai G2 F20 S-TWIN transmission electron microscope (TEM). The TEM images are shown in figure 1 (a), (b) and (c). The GONSs had the largest size (of several square micrometers), and consisted of few layers (less than five). The crimps at the

surfaces and edges resulted from the unstable state of the two-dimensional nanostructure. The GONRs had a large aspect ratio, with a width of approximately 100 nm, which was related to the radius of the raw carbon nanotubes. The GQDs consisted of a few layers, and had a diameter distribution of 3-5 nm. The inset images shown in Figure 1 demonstrated that all of the three samples formed homogeneous and stable aqueous solutions with different colors. The excellent water solubility was due to the large amount of oxygen-containing groups (such as hydroxyl, carboxyl, carbonyl, and epoxy groups) that were present on the edges and planes. Photographs of the GONS, GONR, and GQD hybrid glasses are shown in figure 1 (d), (e), and (f), respectively. The hybrid glasses were transparent to the naked eye, with a thickness of approximately 1.5 mm, and a diameter of 4 cm. The linear transmittances of the GONS, GONR, and GQD hybrid glasses were 60%, 60%, and 78% at 532 nm, respectively (figure 2a). No cracks or any visible sediment were observed. The good mechanical and optical properties of the hybrid glasses doped with graphene materials suggested that they would be suitable for a wide range of applications.

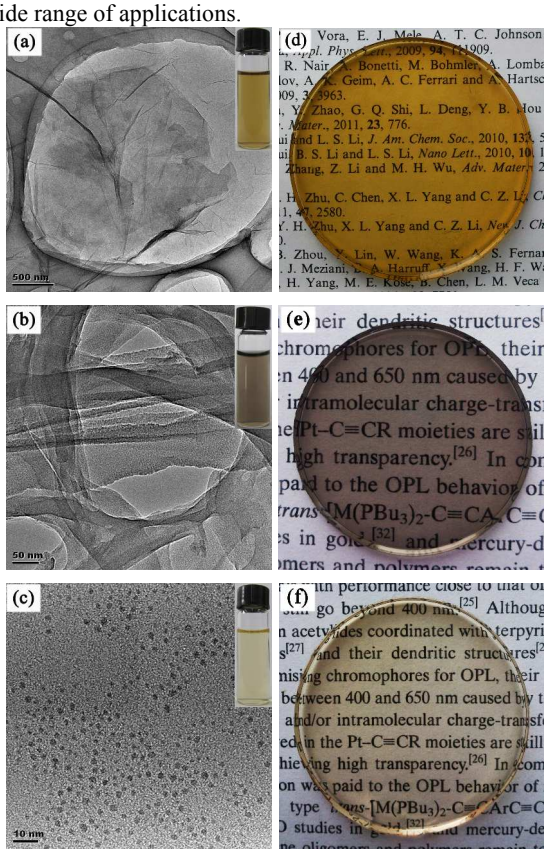

Fig.1 TEM images of (a) GONSs, (b) GONRs, and (c) GQDs, with the inset showing corresponding optical photographs. Photographs of hybrid glasses doped with (d) GONSs, (e) GONRs, and (f) GQDs.

The linear absorption spectra of samples were investigated by a UV spectrophotometer (UV-2450). The results are plotted in figure 2a. The typical absorption peaks for GONSs, GONRs and GQDs were observed at 229, 234 and 300 nm, respectively, which were related to the degree of oxidation and the level of conjugation presented in the system. These results agreed well with previous reports.[20-22] Because graphene materials are known to behave as direct-gap semiconductors, the optical bandgap of the GONSs, GONRs, and GQDs could be determined via the extrapolation of the following equation:[23]

$$\alpha_0 h\upsilon = A(h\upsilon - E_g)^{\frac{1}{2}} \quad (1)$$

where A is a constant, h is Planck's constant, υ is the frequency, α_0 is the weak-field absorption coefficient and E_g is the optical bandgap. By plotting $(\alpha_0 h\upsilon)^2$ against $h\upsilon$, E_g could be obtained via extrapolation of the absorption edge. As shown in figure 2b, the values of E_g for the GONSs, GONRs, and GQDs were 2.75, 3.35, and 3.15 eV, respectively. For graphene materials, the energy bandgap depends on the oxidation and the size. The oxidized sites break the continuity of the π network by forming sp^3-hybridized domains. A direct bandgap can be obtained at these sp^3 domains where the electronic transport barriers appear.[24] First-principle calculation indicates that the oxidized graphene are able to create several eV bandgap, which can be tuned by varying the oxidation level.[25] Moreover, the bandgaps increase when the GONSs were cut into nanoribbons and quantum dots. The finite and irregular edges resulted in strongly localized charge density in the edges. The direct gap is likely to be created at the charge neutrality level and decreases with increasing ribbon width. GQDs show quantum confinement effects primarily originating from the π electron wave functions occupy a potential landscape with strongly repulsive hard wall barriers on the edges.[24,26,27] The energy of a single photon (approximately 2.33 eV) at 532 nm was smaller than the bandgap of the graphene materials. Therefore, when irradiated by 532 nm laser, these graphene materials tended to absorb two photons simultaneously instead of one photon.

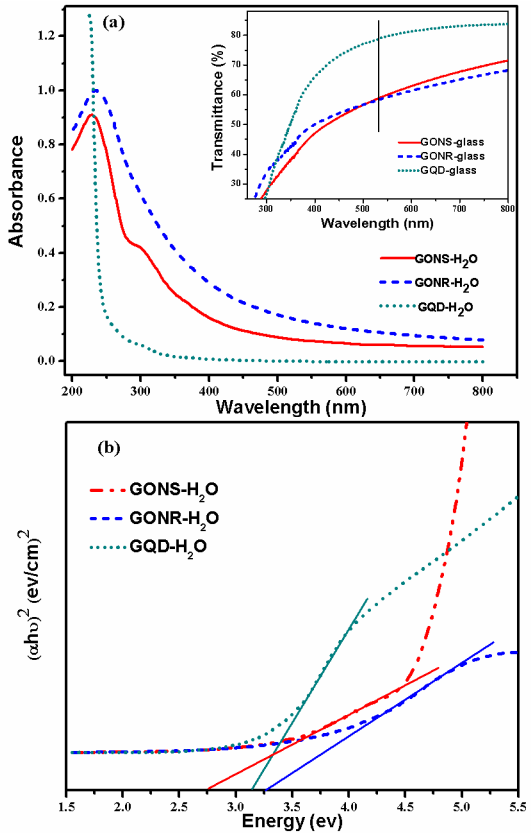

Fig.2 (a) Linear absorption spectra of samples. Inset: linear transmittance spectra of the hybrid glasses. (b) Bandgap evaluation from the plots of $(\alpha_0 h\upsilon)^2$ against energy ($h\upsilon$).

The third-order NLO properties of graphene materials and corresponding hybrid glasses were investigated using Z-scan technique at 532 nm. The laser pulses were generated by a Q-switched Nd:YAG laser with pulse durations and pulse repetition rates of 8 ns, 1 Hz, and 21 ps, 2 Hz. The incident energy was 150 μJ for ns Z-scan and 1.02 μJ for ps Z-scan. The transmittances of the suspensions were determined to be the same as those of the corresponding hybrid glasses.

The ns Z-scan curves for the graphene material suspensions and the hybrid glasses are shown in figure 3.The normalized transmittance decreased rapidly when the sample passed through the focus point. This demonstrated a typical optical limiting effect. The normalized transmittances of the GONS, GONR, and GQD suspensions dropped to 0.56, 0.35, and 0.69, respectively (figure 3a). GONRs showed significantly more prominent NLO effects compared with the GONSs, because of edge-confined effects and the large energy gap. The narrower width and higher oxidation level in GONRs gave rise to a larger energy gap and small-sized localized sp^2 domains, which resulted in slower nonradiative recombination rates and stronger nonlinear absorption of excited states.[9,28] Moreover, defect states increased as the confinement increased in the irregular edges of GONRs. These defect states is likely to generate photo-induced nonlinear absorption similar to FCA when the carriers generated by strong TPA were excited to the defect level under intense irradiation.[29] The assistant nonlinear absorption enhanced the NLO of GONRs. The GQDs showed the weakest NLO performance, because of the weak interaction between the field and the media which resulted from their low concentration and smallest sp^2 domains.[30] The GONS, GONR, and GQD hybrid glasses exhibited enhanced NLO properties, with larger dips compared with the corresponding suspensions (figure 3b). The enhancement mechanism can be described as the effects of the matrix phase.[31] The third-order nonlinear optical susceptibilities of the nanocomposite materials increased with decreases in the dielectric constant of the matrix. Water has a dielectric constant of 78.3, which is much larger than that of silicate glass (1.6). Therefore, the hybrid glasses doped with graphene materials exhibited superior NLO performance.

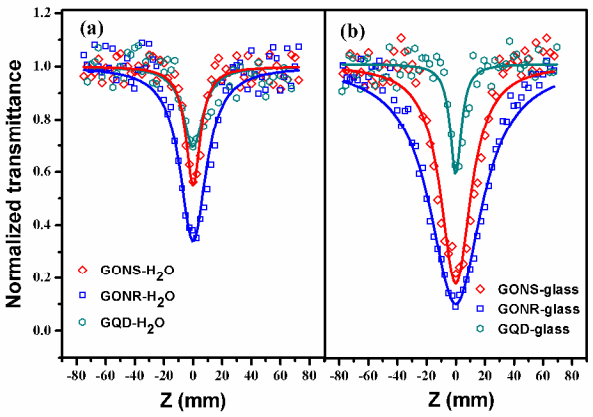

Fig.3 ns z-scan curves for (a) suspensions, and (b) hybrid glasses. The solid lines show theoretical fits to the experimental data.

For graphene materials, nonlinear refraction could be neglected through the closed-aperture Z-scan experiments, and the NLO effect therefore stemmed primarily from nonlinear absorption and/or nonlinear scattering.[32,33] In this work, TPA became the effective nonlinear absorption mechanism when using ns laser pulse. TPA is an instantaneous nonlinearity that involves the simultaneous absorption of two laser photons with assistance of the intermediate state. TPA behavior was strongly affected by the pulse duration and the field intensity. The values of the TPA cross section increased with the broadening of the incident laser pulse and increasing intensity.[30] Therefore, the TPA effect became much weaker when irradiated with short laser pulse that faster than the intersystem transition. On the contrary, SA may play a major role of NLO effect in the ps regime as the lifetime of excited states was much longer than ps.[34] Under the laser irradiation with low energy, the available ground state carriers were depleted, while the excited states became almost occupied, and thus the Pauli exclusion principle came into effect. The probability of optical transitions was therefore reduced significantly, and SA occurred.[35]

The ps Z-scan results for the graphene material suspensions and the hybrid glasses are shown in figure 4. The symmetric peaks were, and the transmission maximum was observed at the focal point, which indicated a typical SA response. SA could be ascribed to ground-state bleaching in the sp^2 regime. Interconnectivity of sp^2 domains resulted in smaller energy gap and fast energy relaxation of hot carriers.[36] The GONSs showed a stronger SA performance compared with the GONRs and the GQDs because of the more large sp^2 domains in the sheets.[13] Similar to the case in the ns regime, the hybrid glasses showed enhanced NLO characteristics, which confirmed the effects of the matrix phase.

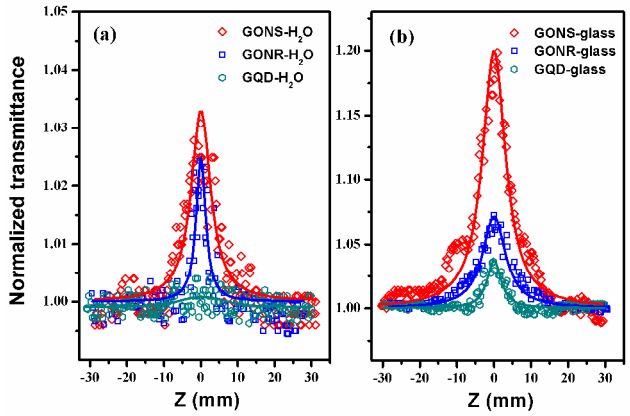

Fig.4 ps z-scan curves for (a) suspensions, and (b) hybrid glasses. The solid lines show theoretical fits to the experimental data.

For a Gaussian laser source, the normalized transmittance can be expressed as:[37,38]

$$T(z)=\frac{1}{\sqrt{\pi}q_0(z,0)}\int_{-\infty}^{+\infty}\ln(1+q_0(z,0)exp(-t^2))dt \quad (2)$$

$$q_0(z,0)=\frac{\alpha I_0 L_{eff}}{1+(z^2/z_0^2)}, \quad (3)$$

$$L_{eff}=\frac{1-\exp(-\alpha_0 L)}{\alpha_0}, \quad (4)$$

here, I_0 is the peak intensity at the focal point, β is the nonlinear absorption coefficient, and L is the thickness of the sample. The

total absorption coefficient is:[39]

$$\alpha = \frac{\alpha_0}{1 + I/I_S} + \beta I \quad (5)$$

where the first term represents SA, while the second term represents the combined effects of TPA, photo-induced nonlinear absorption and/or nonlinear scattering. I is the laser radiation intensity, and I_S is the saturation intensity. The ns and ps Z-scan results fitted using the above formulae are presented in table 1.

Table 1. Nonlinear optical parameters for the samples. β is the nonlinear absorption coefficient and I_s is the saturable intensity.

Samples		ns		ps	
		$\beta\times10^{-10}$ (cm W^{-1})	$I_s\times10^{10}$ (W cm^{-2})	$\beta\times10^{-11}$ (cm W^{-1})	$I_s\times10^{11}$ (W cm^{-2})
suspensions	GONSs	0.59	1.828	-1.02	2.66
	GONRs	0.88	1.244	-0.86	3.18
	GQDs	0.35	1.217	-0.12	10.42
glasses	GONSs	3.64	0.1000	-8.67	0.42
	GONRs	3.97	0.9142	-3.19	1.14
	GQDs	1.57	0.8938	-1.42	1.17

Conclusions

The morphology-dependent bandgap were obtained in graphene materials. The bandgap was increased by cutting GONSs into GONRs and GQDs owning to the edge effect or quantum confinement effects. The third-order NLO properties of these graphene materials and their hybrid glasses were investigated using ns and ps pulses. As the combined effects of nonlinear mechanisms, the NLO process in the ns regime is dominated by RSA, while SA played a major role in the ps regime. The NLO effects of the graphene materials were markedly enhanced when they were introduced into glass matrices with low dielectric constant, which indicated that these hybrid glasses are promising candidates for practical NLO applications.

Acknowledgements

This work was supported by the National Natural Science Foundation of China (No.51172045), Research Fund for the Doctoral Program of Higher Education of China (No.20113514120006) and Natural Science Foundation of Fujian Province (No.2012J0511).

Notes and references

[a] *College of Materials Science and Engineering, Fuzhou University, Fuzhou, 350108, China. E-mail: hbzhan@fzu.edu.cn*
[b] *School of Physical Science and Technology, Soochow University, Soochow, 215006, China.*

1 F. Bonaccorso, Z. Sun, T. Hasan and A. C. Ferrari, *Nat. Photonics*, 2010, **4**, 611.
2 R. S. Singh, V. Nalla, W. Chen, A. T. S. Wee and W. Ji, *ACS nano*, 2011, **5**, 5969.
3 Y. S. Ang and C. Zhang, *Appl. Phys. Lett.*, 2011, **98**, 42107.
4 L. Chua, S. Wang, P. Chia, L. Chen, L. Zhao, W. Chen, A. T. Wee and P. K. Ho, *J. Chem. Phys.*, 2008, **129**, 114702.
5 R. Balog, B. Jorgensen, L. Nilsson, M. Andersen, E. Rienks, M. Bianchi, M. Fanetti, E. Laegsgaard, A. Baraldi, S. Lizzit, Z. Sljivancanin, F. Besenbacher, B. Hammer, T. G. Pedersen, P. Hofmann and L. Hornekaer, *Nat. Mater.*, 2010, **9**, 315.
6 K. P. Loh, Q. Bao, G. Eda and M. Chhowalla, *Nature Chem.*, 2010, **2**, 1015.
7 S. Wang, P. Chia, L. Chua, L. Zhao, R. Png, S. Sivaramakrishnan, M. Zhou, R. G. S. Goh, R. H. Friend, A. T. S. Wee and P. K. H. Ho, *Adv. Mater.*, 2008, **20**, 3440.
8 M. Feng, H. Zhan and Y. Chen, *Appl. Phys. Lett.*, 2010, **96**, 33103.
9 P. Chantharasupawong, R. Philip, N. T. Narayanan, P. M. Sudeep, A. Mathkar, P. M. Ajayan and J. Thomas, *J. Phys. Chem. C*, 2012, **116**, 25955.
10 A. B. Bourlinos, A. Bakandritsos, N. Liaros, S. Couris, K. Safarova, M. Otyepka and R. Zboril, *Chem. Phys. Lett.*, 2012, **543**, 101.
11 Z. Sun, N. Dong, K. Xie, W. Xia, D. Konig, T. C. Nagaiah, M. Sanchez, P. Ebbinghaus, A. Erbe, X. Zhang, L. Alfred, S. Wolfgang, W. Jun and M. Martin, *J. Phys. Chem. C*, 2013.
12 Z. Liu, Y. Wang, X. Zhang, Y. Xu, Y. Chen and J. Tian, *Appl. Phys. Lett.*, 2009, **94**, 21902.
13 Z. Liu, X. Zhao, X. Zhang, X. Yan, Y. Wu, Y. Chen and J. Tian, *J. Phys. Chem. Lett.*, 2011, **2**, 1972.
14 X. Q. Zheng, M. Feng and H. B. Zhan, *J. Mater. Chem. C*, 2013, **1**, 6759.
15 S. Husaini, J. E. Slagle, J. M. Murray, S. Guha, L. P. Gonzalez and R. G. Bedford, *Appl. Phys. Lett.*, 2013, **102**, 191112.
16 G. Zhou and W. Wong, *Chem. Soc. Rev.*, 2011, **40**, 2541.
17 G. Zhou, W. Wong, C. Ye and Z. Lin, *Adv. Funct. Mater.*, 2007, **17**, 963.
18 G. Zhou, W. Wong, D. Cui and C. Ye, *Chem. Mater.*, 2005, **17**, 5209.
19 G. Zhou, W. Wong, Z. Lin and C. Ye, *Angew. Chem. Int. Ed.*, 2006, **45**, 6189.
20 D. C. Marcano, D. V. Kosynkin, J. M. Berlin, A. Sinitskii, Z. Sun, A. Slesarev, L. B. Alemany, W. Lu and J. M. Tour, *ACS nano*, 2010, **4**, 4806.
21 D. V. Kosynkin, A. L. Higginbotham, A. Sinitskii, J. R. Lomeda, A. Dimiev, B. K. Price and J. M. Tour, *Nature*, 2009, **458**, 872.
22 D. Pan, J. Zhang, Z. Li and M. Wu, *Adv. Mater.*, 2010, **22**, 734.
23 P. Chantharasupawong, R. Philip, T. Endo and J. Thomas, *Appl. Phys. Lett.*, 2012, **100**, 221108.
24 Z. Luo, P. M. Vora, E. J. Mele, A. C. Johnson and J. M. Kikkawa, *Appl. Phys. Lett.*, 2009, **94**, 111909.
25 J. Yan, L. Xian and M. Y. Chou, *Phys. Rev. Lett.*, 2009, **103**, 86802.
26 X. Li, X. Wang, L. Zhang, S. Lee and H. Dai, *Science*, 2008, **319**, 1229.
27 G. Lee and K. Cho, *Phys. Rev. B*, 2009, **79**, 165440.
28 X. Jiang, L. Polavarapu, S. T. Neo, T. Venkatesan and Q. Xu, *J. Phys. Chem. Lett.*, 2012, **3**, 785.
29 T. G. Pedersen, C. Flindt, J. Pedersen, N. A. Mortensen, A. Jauho and K. Pedersen, *Phys. Rev. Lett.*, 2008, **100**, 136804.
30 C. Wang, P. Zhao, Q. Miao, Y. Sun and Y. Zhou, *J. Phys. B: At. Mol. Opt. Phys.*, 2010, **43**, 105601.
31 Y. Y. Sun, B. H. Yang, G. Z. Guo, H. Shi, Y. Tian, M. H. He, J. C.

Chen, Y. Q. Liu, G. Z. Zhao and Q. J. Zhang, *EUR PHYS J-APPL PHYS*, 2011, **56**.

32 J. Wang, Y. Hernandez, M. Lotya, J. N. Coleman and W. J. Blau, *Adv. Mater.*, 2009, **21**, 2430.

33 N. Liaros, P. Aloukos, A. Kolokithas-Ntoukas, A. Bakandritsos, T. Szabo, R. Zboril and S. Couris, *J. Phys. Chem. C*, 2013, **117**, 6842.

34 A. Karatay, C. Aksoy, H. G. Yaglioglu, A. Elmali, U. Kurum, A. Ates and N. Gasanly, *J. Opt.*, 2011, **13**, 75203.

35 T. Winzer, A. Knorr, M. Mittendorff, S. Winnerl, M. Lien, D. Sun, T. B. Norris, M. Helm and E. Malic, *Appl. Phys. Lett.*, 2012, **101**, 221115.

36 X. Zhao, Z. Liu, W. Yan, Y. Wu, X. Zhang, Y. Chen and J. Tian, *Appl. Phys. Lett.*, 2011, **98**, 121905.

37 M. Sheik-Bahae, A. A. Said, T. Wei, D. J. Hagan and E. W. Van Stryland, *IEEE J QUANTUM ELECT*, 1990, **26**, 760.

38 Y. Gao, X. Zhang, Y. Li, H. Liu, Y. Wang, Q. Chang, W. Jiao and Y. Song, *Opt. Commun.*, 2005, **251**, 429.

39 M. Hercher, *Applied Optics*, 1967, **6**, 947.

The nonlinear optical properties of nonzero-bandgap graphene materials and the corresponding hybrid glasses were strongly affected by the laser duration.